*Int. J. Electrochem. Sci.*, 8 **(2013)** 1079 - 1094

International Journal of
ELECTROCHEMICAL
SCIENCE
www.electrochemsci.org

# Microbially Induced Corrosion Rate Determination Applying Clark Amperometric Sensor

*R. Zlatev*[1,*], *M. Stoytcheva*[1], *S. Kiyota*[2], *M. Ovalle*[3], *B. Valdez*[1], *R. Ramos*[1]

[1] Engineering Institute, Autonomous University of Baja California, Blvd. B. Juárez s/n, Mexicali, Baja California, México, CP 21280
[2] Honeywell Airspace, Ind. Park el Vigia II Carr. San Luis, Mexicali CP 21395
[3] CNyN, UNAM, Ensenada, Km 107 Carretera Tijuana-Ensenada, Apdo. Postal 14, CP. 22800 Ensenada, B.C. México
[*]E-mail: roumen@uabc.edu.mx

*Received:* 19 November 2012 / *Accepted:* 14 December 2012 / *Published:* 1 January 2013

The Clark amperometric oxygen sensor was applied for specific microbially induced corrosion (MIC) rate determination promoted by the bacterial strain *Acidithiobacillus ferrooxidans* which catalyzes the iron oxidation by the dissolved oxygen (DO) accelerating thus the corrosion process. The corrosion acceleration of UNS G1020 carbon steel provoked by the bacteria in aqueous media with pH from 2 to 6 ($H_2SO_4$) was evaluated by the slope increase of the curve: DO consumption vs. time in the presence of bacteria. A background subtraction was done to avoid the abiotic oxygen consumption interference. The Potentiodinamic Polarization was applied for general corrosion rate determination at abiotic conditions used as a reference for the corrosion acceleration determination provoked by the bacteria. Values from 0.017 to 8.68 mm year$^{-1}$ were obtained for the bacterial corrosion rate provoked by the bacterial strain *Acidithiobacillus ferrooxidans* in the mentioned pH interval, while the general corrosion rates were in the range from 0.0147 to 1.766 mm year$^{-1}$ respectively, which represents corrosion acceleration between 1.16 and 4.91 times for the pH in the range from 6 to 2 respectively in unstirred aqueous media.

**Keywords:** Microbial Influenced Corrosion (MIC), *Acidithiobacillus ferrooxidans*, MIC rate specific determination

## 1. INTRODUCTION

Electrochemical techniques such as Linear Polarization Resistance (LPR), Potentiodinamic Polarization (PDP), Electrochemical Noise (EN), and Electrochemical Impedance Spectroscopy (EIS) [1-6] are widely applied for the corrosion rate (CR) determination. These techniques however do not allow specific evaluation of the corrosion acceleration (total corrosion rate augmentation) caused by

corrosion promoting bacteria strains such as *Acidithiobacillus ferrooxidans* for example which is able to provoke sever damages of the steel industrial equipment. The distinction of the microbially induced corrosion (MIC) rate which may largely exceed the general corrosion one [7-14] is of a great importance for adequate MIC inhibitor/suppressor choice.

The mentioned electrochemical techniques are very simple in their application yielding reliable real time results for the general corrosion rate (CR) at abiotic conditions. For example the CR is determined from the LPR results [1] employing the equation:

$$CR = K\,(i_{corr} / \delta)\,EW \qquad (1)$$

where: K = constant, $EW$ = equivalent mass; $\delta$ = density; $i_{corr}$ = corrosion current.

The corrosion current could be calculated from the potentiodynamic plot:

$$I_{corr.} = \beta / R_p \qquad (2)$$

where: $\beta$ = Tafel slope; $R_p$ = polarization resistance.

Similar to LPR the Electrochemical Noise (EN) technique yields the Noise Resistance $R_n = \sigma_V/\sigma_I$, (where $\sigma_V$ and $\sigma_I$ are the standard deviations of the potential and the current respectively) instead of the polarization resistance. Its replacement in the equation: $i_{corr} = \beta/R_p$ instead of $R_p$ results in the $i_{corr}$ which substituted it in the equation (2) yields the CR. The potentiodynamic polarization technique (Tafel plot registration) allows direct and simple determination of the corrosion current and hence the CR.

However, since the MIC is attributed to the bacterial metabolic activity within a bacterial biofilm which existence is the main condition for the MIC occurrence [15], the MIC rate determination and its distinction from the general corrosion rate require specific methods to be applied. For example Sahrani et al. [16] applied the EIS to determinate the polarization resistance decrease of stainless steel caused by corrosion provoking sulphate-reducing bacteria. This method however does not allow a precise distinguishing of the MIC rate. Schnaitman et al. [17] reported a specific method for MIC rate determination caused by the bacterial strain *Acidithiobacillus ferrooxidans*. This method is based on $Fe^{2+}$ concentration monitoring, an intermediate product of the first stage of the corrosion process: Fe oxidation to $Fe^{2+}$. The $Fe^{2+}$ concentration was determined applying the Lowry's spectrophotometric method [18] taking samples periodically. The complicated and long measuring procedure did not allow the wide application of this method.

The strain *Acidithiobacillus ferrooxidans* finds a large industrial applications, such as: sulfide minerals bioleaching in copper metallurgy, uranium and other heavy metals uptake during waste water [19] and sulfur containing coals treatment [20], etc. The great industrial application of this bacterial strain due to its specific properties is combined however with its devastating drawback: to be one of the most corrosive bacterial strains, provoking sever deterioration and degradation of the steel industrial equipment [21]. The presence of *Acidithiobacillus ferrooxidans* may provoke an extreme increase of the corrosion rate due to their ability to catalyze the iron oxidation by dissolved oxygen in acid media yielding oxides or hydroxides [18, 22] or formation of deposits creating concentration

galvanic cells, all these favored by the strong bacteria ability to form biofilm on many solid surfaces, which is the main condition for MIC appearance, as stated by Zuo and Duan [14]. The biofilm represents an aggregation of bacteria, enclosed in a matrix consisting of a mixture of: polymeric compounds generally referred to extracellular polymeric substances (EPS) produced by microorganisms, as well as primarily polysaccharides, proteins, nucleic acids, lipids and humic substances [23]. The key functions of EPS comprise the mediation of the initial attachment of cells to different surfaces. The biofilm formation not only supports the corrosion but serves as an impermeable barrier [24, 25] even for the heavy metals loaded effluents and the antibacterial cleaning solutions [18, 26]. Songmei Li et al. [27] presented a detailed study on the *Acidithiobacillus ferrooxidans* biofilm formation on A3 steel and its influence on the MIC rate, evaluated applying electrochemical methods.

Factors as: high bacterial cell concentrations and low pH oxygen rich aqueous media are combined with the *Acidithiobacillus ferrooxidans* strong fixation and biofilm formation ability in the common industrial environment. This combination favors the MIC which requires the development of specific and simple method for *Acidithiobacillus ferrooxidans* MIC rate determination which is of importance for adequate MIC inhibitor application to protect the industrial equipment.

Many mechanisms were proposed till now for the iron oxidation at abiotic conditions. Schrenk and Kanematsu [24, 28] for example stated that the iron oxidation occurs by two different mechanisms depending on the pH: in acid media: a spontaneous metal dissolution occurs with hydrogen formation:

$$Fe + 2H^{+} \rightarrow Fe^{2+} + H_2 \quad (3)$$

while in alkaline media the ferrous iron ($Fe^{2+}$) is oxidized chemically to ferric iron ($Fe^{3+}$) with oxygen participation able to form hydroxide and complexes with organic compounds or to be reduced chemically back to ferrous iron by hydrogen sulfide:

$$4Fe + 6H_2O + 3O_2 \rightarrow 4Fe(OH)_3 \quad (4)$$

Another mechanism was proposed by Drazic [29] and Plonski [30] who stated that the iron oxidation (corrosion) occurs in several steps which differ according to the pH but the first step is always the following:

$$Fe + H_2O \leftrightarrow FeOH_{ads}^{+} + H^{+} + e^{-} \quad (5)$$

Then in acidic to neutral media the species $FeOH_{ads}^{+}$ are formed by loosing electron and this step determines the rate of the Fe oxidation (corrosion rate)

$$FeOH_{ads} \rightarrow FeOH_{ads}^{+} + e^{-} \quad (6)$$

and finally the oxidized iron goes into solution via the reaction:

$$FeOH_{ads}^{+} + H^{+} \leftrightarrow Fe^{2+} + H_2O \quad (7)$$

The reaction (7) which is part of the so called Bockris-Drazic-Despic mechanism (BDD) [31-33] can be branched into many variants. None of them however have been experimentally verified till now.

In presence of the bacteria *Acidithiobacillus ferrooxidans* in acidic aqueous media however another mechanism begins to contribute to the iron dissolution, accelerating the corrosion process. The bacteria use the existing proton gradient between the pH-neutral bacterial cytoplasm and the acid external environment to generate energy, catalyzing the iron oxidation by the dissolved oxygen (DO). The latter acts as a terminal electron acceptor to produce water while the hydrogen ions are consumed on the cytoplasm side of the bacterial cell membrane. *Acidithiobacillus ferrooxidans* possess the enzyme ironoxidase, allowing metabolizing the metal iron and ferrous iron to iron oxides and hydroxides according to the equations (8 - 12) [21, 24, 28, 34]. The formed $Fe^{3+}$ may served as an inhibitor of the bacterial Fe and $Fe^{2+}$ oxidation diminishing thus the MIC corrosion rate, but this phenomenon occurs at high ferric iron concentrations only, as stated by Lazaroff [35].

$$Fe \rightarrow Fe^{2+} + 2e^{-} \quad (8)$$

$$4Fe^{2+} + O_2 + 4H^{+} \rightarrow 4Fe^{3+} + 2H_2O \quad (9)$$

$$4Fe^{2+} + SO_4^{2-} + 2H_2O + 2H^{+} \rightarrow 3Fe(OH)_2 + FeS \quad (10)$$

$$Fe_2(SO_4)_3(aq) + 6H_2O \rightarrow 2Fe(OH)_3(aq) + 3H_2SO_4(aq) \quad (11)$$

$$Fe^{2+} \rightarrow Fe^{3+} + e^{-} \quad (12)$$

The iron oxidation by *Acidithiobacillus ferrooxidans* always occurs with DO consumption which can be used as a very specific measure of the rate of the MIC provoked by this strain. The DO consumption due to abiotic parallel processes can be taken into account by background subtraction after blank experiments at abiotic conditions. The goal of the present work, as a continuation of a previous author's work [36], is to apply the specific method based on Clark type amperometric sensor for real time determination of UNS G1020 carbon steel corrosion acceleration provoked by the high concentrations of the bacteria *Acidithiobacillus ferrooxidan* in acidified ($H_2SO_4$) aqueous media in pH interval from 2 to 6 over the time. The potentiodinamic politicization were applied as reference methods to determine the general corrosion rate at abiotic conditions.

## 2. EXPERIMENTAL

### *2. 1. Regents*

All the reagents were of analytical grade from Merck and Sigma and deionized water produced by Milli Q reverse osmoses installation (Millipore) was employed for all the solutions preparation. Lawry test kit from Sigma was used for the bacterial protein concentration determination together with the Schnaitman's spectrophotometric method [17].

*2. 2. Specimen preparation*

A piece of two inches in diameter UNS G1020 carbon steel tube commonly used in industrial installations with a surface of 200 $cm^2$ on both sides was used as a test specimen in all the experiments. UNS G1020 is a low carbon steel having a composition: C 0.20%, Si 0.25%, Mn 0.45%, P 0.04%, S 0.04%, and Fe - the balance percentage suitable for machine parts and welded component widely used for industrial equipment not requiring high strength [37]. The UNS G1020 steel composition does not include heavy metals which strongly decrease the *Acidithiobacillus ferrooxidans* metabolism during its growing as reported by Magnin et al. [38]. The specimen surfaces were polished with abrasive sandpaper # 400 before every experiment.

*2. 3. Electrochemical instrumentation*

The potentiodynamic polarization (PDP) (Tafel plot) performed from -0.7 VOCP to +0.7 VOCP with a scan rate of 0.5 mV/s was applied to evaluate the corrosion rate in acid ($H_2SO_4$) water solutions with pH from 2 to 6 at room temperature. A PC4 FAS1 (Gamry Instruments Inc.) potentiostat/galvanostat controlled by CMS100/CMS300 software coupled to a conventional three-electrode electrochemical cell with a Ag/AgCl/3M KCl reference electrode and graphite bar counter electrode were used.

In all the electrochemical experiments UNS G 1020 carbon steel coupons mounted in epoxy resin having exposed area of 0.18 $cm^2$ were employed. Prior to the electrochemical tests the samples surfaces were polished with sand paper from 240 to 1200 grade and then cleaned with acetone to remove eventual oil traces.

The same equipment was employed for open circuit potential (OCP) monitoring up to its stabilization.

*2. 4. Dissolved oxygen consumption monitoring setup*

The DO consumption determinations were performed in 5 L cylindrical acrylic container (measuring cell), with 20 cm internal diameter, equipped with a magnetic stirrer bar at the bottom, closed with an O-ring sealed cover at the top (see Fig. 1).

The internal part of the cover was conically shaped preventing the sticking of air bubbles on its surface. A semispherical front and Clark type oxygen probe was mounted across the measuring cell to prevent the air bubbles sticking on its membrane. Au microwares distributed uniformly in acrylic resin forming Au micro spots on the semispherical probe body surface were employed to form the sensor multicathode. The Clark probe was connected to a low current potentiostat model Z 54 (ZenitLab, Bulgaria) equipped with a current compensation circuit allowing increasing the current sensitivity after the compensation and measurement of extremely small DO concentration changes. A special noise reduction circuit developed by the authors earlier [39] increased the signal to noise ratio at the increased sensitivity allowing registration of smooth curves.

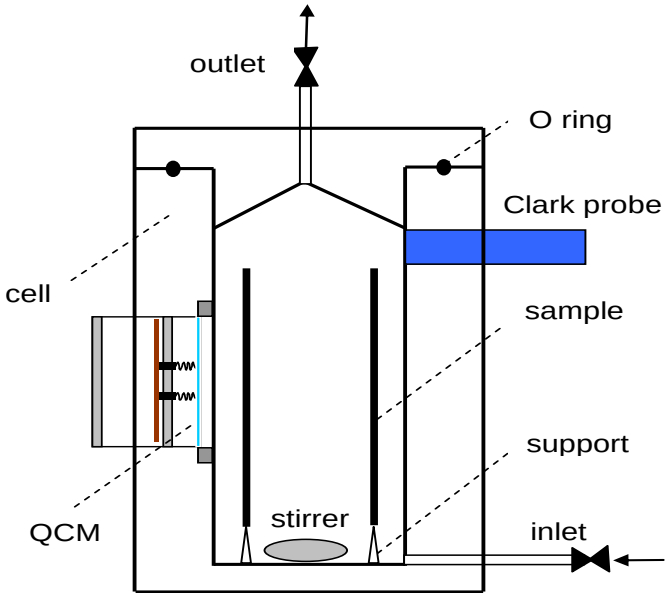


**Figure 1**. Measuring cell construction

*2. 5. Bacterial growth monitoring*

The bacterial strain *Acidithiobacillus ferrooxidans* – DSM 583 was obtained from the German Collection of Microorganisms and Cell Cultures. The widely used media "9K" with pH 1.4 proposed by Tuovinen et al. [40], was employed for the *Acidithiobacillus ferrooxidans* culture development in thermostated by air at 30$^{o}$C 0.5 L reactor under agitation with 100 rpm. The bacteria growth was monitored by the application of the o-phenantroline based spectrophotometric method [41] for $Fe^{2+}$ concentration determination. A potentiometric method based on the Red/Ox potential monitoring [42] was also applied for real time determination of the $Fe^{2+}/Fe^{3+}$ concentration ratio according to the Nernst equation (6):

$$E = E^{o} + \frac{RT}{F} \ln \frac{[Fe^{3+}]}{[Fe^{2+}]} \qquad (12)$$

where $E$ is the $Fe^{2+}/Fe^{3+}$ couple redox potential, $E^{o}$ is the standard $Fe^{2+}/Fe^{3+}$ couple redox potential, $R$ is the gas constant, $T$ is the temperature, $F$ is the Faraday constants and $[Fe^{3+}]$ and $[Fe^{2+}]$ are the ionic concentrations at equilibrium.

The redox potential value corresponding to the end of the exponential part of the *Acidithiobacillus ferrooxidans* growth curve in "9K" media was experimentally determined to be +830 mV vs. SCE. The protein concentration was determined by optical density measurement of the bacterial culture using a preliminary built calibration curve in coordinates: protein concentration

determined by the Lowry method [18] adapted to *Acidithiobacillus ferrooxidans* [43] vs. light absorption at 330 nm.

### *2.6. Acidithiobacillus ferrooxidans biofilm formation monitoring methodology and setup*

The biofilm formation is of a great importance for the MIC appearance and development and that is why various methods have been developed till now for its monitoring. Bott [44] described several techniques using: weight measurement, infrared light absorbance measurements of transparent surface, electrical resistance measurement, and heat transfer resistance measurement. Tribollet [45] employed the mass transport resistance increase affecting the diffusion current. All the mentioned methods are very complicated and applicable at specific cases only.

The authors developed earlier [46] a quantitative method based on quartz crystal microbalance (QCM) application for real time *Acidithiobacillus ferrooxidans* biofilm formation rate monitoring. This method was properly modified and applied in this study employing two types of QCM crystals: covered by UNS G 1020 carbon steel and covered by gold. One inch in diameter, 5 MHz QCM quartz crystal (Inficon/Maxtek) was modified by a vacuum deposition of 20 nm (+/-20%) steel layer on the Ti adhesion layer of the QCM quartz crystal using a UNS G 1020 carbon steel target. The QCM crystal was placed as a substrate in a high vacuum chamber at room temperature with a crucible containing the material (UNS G1020) to be deposited. A resistive heating source was used to heat the crucible causing the material to evaporate and condense on substrate and all exposed cool surfaces of the vacuum chamber as well. The difference between the deposited film composition and that of the UNS G 1020 carbon steel target resulted from the different evaporation temperatures of the alloys ingredients was ignored because this carbon steel does not contain ingredients affecting the bacteria metabolism.

The modified QCM quartz crystals were exposed to *Acidithiobacillus ferrooxidans* bacterial culture with known concentration (expressed by its optical density) in $H_2SO_4$ water solutions with pH in the range from 2 to 6 (Fig. 1). The QCM frequency proportional to the mass of the biofilm formed on the quartz crystal was monitored (Fig. 2) and the mass was calculated applying the Sauerbrey equation [47]:

$$\Delta F = -C_f \Delta m \qquad (13)$$

where $\Delta F$ is the frequency change in Hz; $C_f$ is the sensitivity factor of the quartz crystal in Hz $ng^{-1}$ $cm^2$; $\Delta m$ is the mass change per unit area in g $cm^{-2}$. According to the data provided by the crystal producer $C_f$ = 0.0566 Hz $ng^{-1}$ $cm^2$. To avoid the interference of the abiotic corrosion of the UNS G1020 carbon steel film deposited on the QCM crystal, parallel measurements were made employing QCM crystals covered by gold.

*2. 7. Real time specific MIC rate determination methodology*

In all the experiments the specimen of UNS G1020 carbon steel tube of 200 $cm^2$ total surfaces was put on plastic supports inside the measuring cell shown in Fig. 1 entirely filled with $H_2SO_4$ aqueous solution with appropriated pH in the range from 2 to 6. To increase the initial DO concentration preventing thus the MIC to be limited by the oxygen diffusion the testing solution was preliminary aerated by stirring at 500 rpm at open air during two hours before every experiment. The oxygen solubility in water at 1 atm pressure and 25$^o$C is known to be 42 mg $L^{-1}$ and the oxygen partial pressure in the air is 0.2 atm. At these conditions the DO equilibrium concentration in still deionized water in contact with the air was calculated to be 42x0.2 = 8.4 mg $L^{-1}$ according to the Henry law [48]: ($p = ck_H$ with $k_H$ = 769.2 L atm $mol^{-1}$). The real concentration of DO however depends not only on the temperature, but on the dissolved substances concentrations as well. For example oxygen saturation concentrations up to 11.8 mg $L^{-1}$ was achieved in the solution with pH 2 at open air at 500 rpm.

After the testing solution aeration, the measuring cell was carefully closed without air bubbles inside attached to its wall. The Clark probe current was first compensated to zero and the preamplifier sensitivity was increased to its maximum possible, allowing thus the registration of very small changes of the DO concentration. After the Clark probe signal stabilization the bacterial culture was added into the solution through the cell inlet (see Fig. 1) and the extra volume was removed through the cell outlet. No stirring was applied during the DO monitoring simulating thus the basic MIC conditions.

## 3. RESULTS AND DISCUSSION

*3.1 Oxygen probe calibration plot building and response time determination*

The approach proposed in this work is based on the MIC rate determination by DO consumption evaluated by the Clark probe current employing a calibration plot in coordinates: Clark Probe Current – DO concentration. The easiest way for the calibration plot construction was the Clark probe response registration in two points: first in deionized water with DO = 0 achieved by $Na_2SO_3$ addition and second in non-stirred deionized water held 24 hours in contact with the air up to a equilibrium to be established at room temperature. The calibration plot is presented in Figure 2 (right).

Since the slope of the curve in coordinates: bacterial *DO concentration (Clark probe current) - time* is the measure of the MIC rate, the response time of the oxygen probe is of an importance for the results precision. As known, the falling Clark probe response time is always longer than the rising one because of the longer time necessary to be consumed the already accumulated DO in the volume of the internal Clark probe solution.

The Clark probe falling response time depends on parameters as: Clark probe indicator electrode real surface, total volume of the probe internal solution, the electrolyte layer thickness above the indicator electrode and the membrane thickness [49]. The application of semispherical front end probe with uniformly distributed multi-cathode as indicator electrode situated at small distance from the plastic membrane employing a small internal solution volume allows the achievement of shorter falling response time.

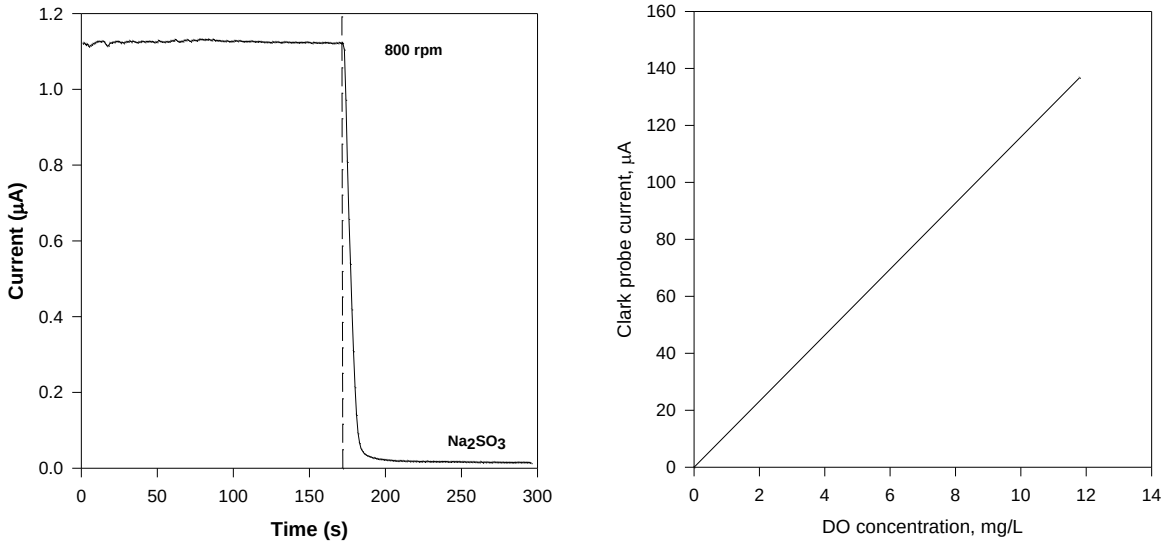


**Figure 2**. Clark oxygen probe falling response time (left) and Clark oxygen probe calibration plot for $H_2SO_4$ solution with pH = 2 (right)

A noise suppression module based on the proposed by the authors specific approach was applied for more precise results [39]. The falling probe response determination methodology reported by the authors earlier [49] based on $Na_2SO_3$ addition was employed (Fig. 2) and response time down to 5% of the maximal value (95% of the sensor range signal change) was determined to be 10.81 s.

*3.2. Biofilm formation monitoring*

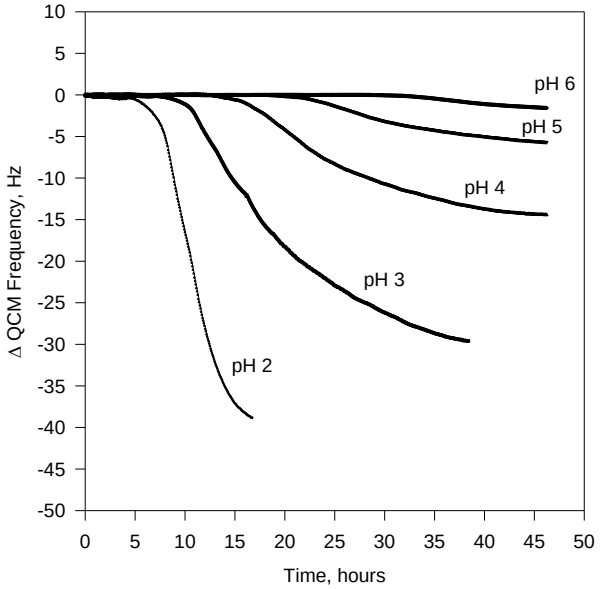


**Figure 3**. Real time QCM curve of *Acidithiobacillus ferrooxidans* biofilm formation on gold coated QCM crystals at pH in the range from 2 to 6. Bacteria addition at time = 0

Since the biofilm existence is the main condition for MIC appearance, the determination of the beginning of its formation is of great importance to determine the beginning of MIC. For this purpose a QCM was applied to monitor the biofilm formation over time and the obtained results for different pH values are shown in Fig. 3. The results obtained with the gold coated QCM quartz crystals (see Fig. 3) were found to be more reliable because of the interference of the abiotic corrosion making the results obtained with UNS G1020 carbon steel coated QCM irreproducible.

As presented in Fig. 3, the biofilm formation begins after a latency period starting with the bacterial culture addition and depending on pH at constant bacterial cell concentrations (optical density): closer the pH value to the optimal value of 1.4, shorter the latency. Data for the latency periods presented in Table 1 were obtained from the crossing points of the continuation of the falling part of the corresponding QCM curves with the zero line ($\Delta F = 0$).

**Table 1**. Biofilm formation latency period as a function of the pH

| pH | Latency, hours | pH | Latency, hours |
|---|---|---|---|
| 2 | 7.1 | 5 | 21.6 |
| 3 | 9.7 | 5 | 33.2 |
| 4 | 15.4 | | |

A small fall followed by a small semi-plateau occurs on the QCM frequency/time plot immediately after the addition of the bacterial culture to the measuring cell resulting from the immediate bacterial physical attachment (fixation) to the QCM crystal surface. Once attached, the bacteria begin the biofilm formation from its metabolism products and this process occurs much more slowly taking hours and even days depending on the bacterial cell concentration and the environmental conditions.

### *3.3. Blank measurement by Clark type amperometric probe in bacteria free media*

According to the iron corrosion mechanism proposed by Schrenk and Kanematsu [24, 28] mentioned above, the DO is involved in the corrosion processes in alkaline media only, while the iron dissolution occurs with $H_2$ generation in acidic media and it could not be expected any oxygen consumption in acidic media at abiotic conditions. On the other hand however, since the BDD mechanism is controversial to the Schrenk and Kanematsu one, blank experiments were carried out registering the DO consumption in acid media with pH from 2 to 6 at the absence of bacteria. In Fig. 4 are shown the curves: oxygen concentration vs. the time during the first 5 minutes of the contact of the sample with the aqueous solutions while the full curves for pH = 2 and pH = 6 are shown in Fig. 6.

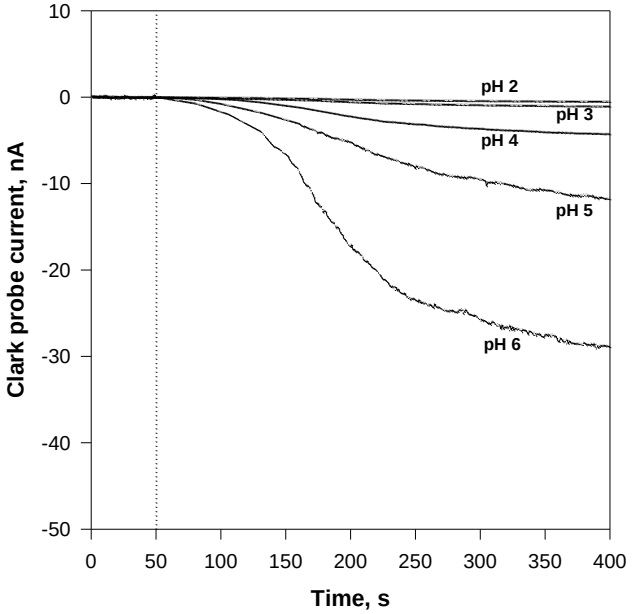


**Figure 4**. Blank experiments: Clark probe current (oxygen consumption) vs. time curves in bacteria free acidic media with pH from 2 to 6 after initial current compensation to zero.

The registered curves fit well to the statements of Schrenk and Kanematsu [24, 28] at very acid media only (pH<3), but considerable DO consumption was registered at higher pH values, increasing with pH. This fact leads to the conclusion that the mentioned above BDD mechanism [31-33] explain better the corrosion process especially for pH>3: higher the pH value, higher the DO consumption in bacteria free media. For the purpose of the blank determination the results obtained at pH = 2 and pH = 3 can be ignored because of their negligible values.

*3.4. General CR determination by Potentiodynamic Polarization (PDP) application*

The Potentiodynamic Polarization (PDP) was applied for the general corrosion rate determination in bacteria free media to be compared with the CR results obtained in the presence of bacteria with the Clark probe employment i.e. to determine the corrosion acceleration caused by MIC. First, the open circuit potential (OCP) for every pH value in the range from 2 to 6 was determined to define the potential sweeps ranges (Fig. 5 left). While the OCP was established rapidly for the pH 2 and pH 3 causing a stable and flat horizontal curve along time, the OCP for pH>3 could not equilibrate completely within 2 hours starting from almost 2 times more positive potential compared with the values obtained at pH<3. The OCP/time curves for pH 5 and pH 6 achieved their equilibrate value after more than 7 and more than 10 hours respectively (not shown in the figure to avoid the extreme scale expansion) obviously caused by the complicated corrosion mechanism with increased influence of the DO.

The Tafel plots for UNS G 1020 in diluted $H_2SO_4$ solutions with pH from 2 to 6 showed that the pH 3 is a division point; the corrosion potential changes drastically for pH>3 and the Tafel plots are grouped in two groups depending on the pH, as seen from Fig. 5 right. The groups formation occurs with the curves registered immediately after the specimen's immersion, as well with the curves registered one hour after the specimen's immersion. This fact can be explained with the general attack involving the continual dissolution of the UNS G 1020 at pH 2 and 3 dictated by the hydrogen cathodic reaction $2H^+ + 2e \rightarrow H_2$ while for less acidic media (pH 4, 5, and 6) the reduction of the dissolved oxygen is the predominant cathodic process in the corrosion mechanism: $O_2 + 2H_2O + 4e^- \rightarrow 4OH^-$. The anodic branches of the Tafel plots are affected by the acidic media: lower the pH, higher the current density while the cathodic branches are strongly affected by the DO and $H^+$ reduction that limit the current at more negative potentials.

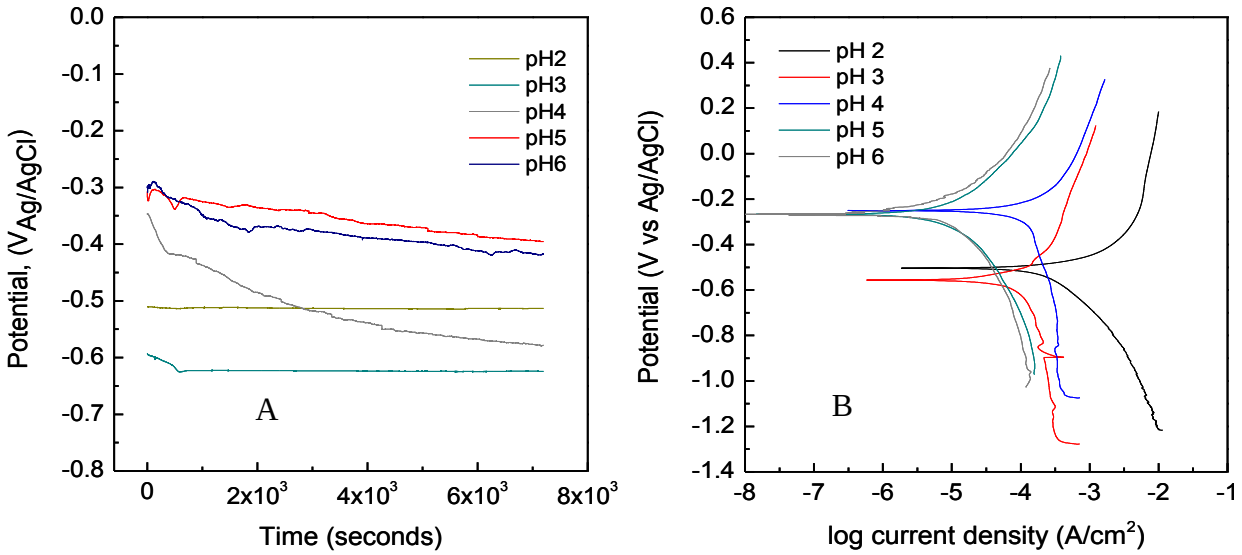


**Figure 5**. OCP (A) and Tafel plots (B) of UNS G 2010 electrode in bacteria free $H_2SO_4$ media with pH in the range from 2 to 6.

Data for some electrochemical parameters employed for the corrosion rate calculation by Tafel plots extrapolation and the corresponding corrosion rate values, evaluated by CMS100/CMS300 software application are presented in Table 2.

**Table 2**. Corrosion rate of UNS G1020 in acid media (pH from 2 to 6, $H_2SO_4$)

| pH | $-E_{corr}$, mV | Current density $i_{corr}$ $\mu A\ cm^{-2}$ | Corrosion rate $mm\ y^{-1}$ |
|---|---|---|---|
| 2 | 504 | 152 | 1.766 |
| 3 | 556 | 49.2 | 0.572 |
| 4 | 362 | 6.05 | 0.070 |
| 5 | 399 | 3.2 | 0.037 |
| 6 | 378 | 1.27 | 0.0147 |

Applying the Kopliku and Bazzoni classification [50] to the results obtained for the different pH values shown in Table 2, one can conclude that the CR is very low at pH = 5 and 6, low at pH = 4, while at pH = 3 and especially at pH = 2 it can be characterized as sever.

### *3.5. MIC rate determination*

The MIC rate was evaluated by the DO consumption rate: the slope ($\Delta C_{ox}/\Delta t$) of the DO concentration vs.the time (Clark probe current - time) curves taking into account that 1 mol oxygen oxidized 4 moles of iron (Eq. 9). Since the biofilm formation is the most important condition of MIC appearance, the slope of the curve after the latency period termination (when the biofilm is very thin but already formed) was employed for the MIC rate evaluation. The latency period duration depends on pH: higher the pH value, longer the latency period, as seen from Fig. 3. A background subtraction was made using the data presented in Fig. 4 to eliminate the oxygen consumption interference caused by the corrosion occurring at abiotic conditions allowing precise and specific determination of the MIC rate provoked by the bacterial strain *Acidithiobacillus ferrooxidans*.

The Clark probe current vs. the time curves registered at the presence of bacteria together with the blank curves registered at abiotic conditions at pH 2 and pH 6 are presented in Fig. 6. The slope $\mu$ which is the measure of the MIC rate was determined after background subtraction according to the equation: $\mu_x = \alpha_x - \beta_x$ where $\alpha_x$ is the total slope of the DO concentration vs. time curve at pH = X (X = 2 to 6) and $\beta_x$ is the slope of the blank curve at pH = X and abiotic conditions.

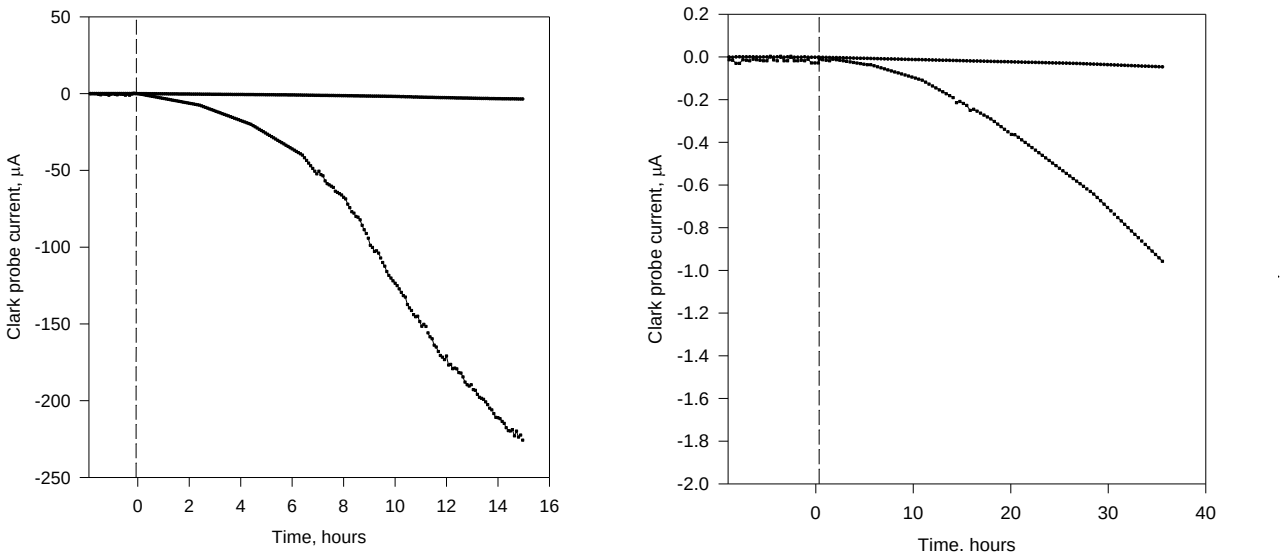


**Figure 6**. Oxygen consumption vs. time curves in the presence of bacteria ($\alpha$) and blank experiments curves ($\beta$) all registered in acidic media with pH 2 (left) and pH 6 (right). The initial Clark probe current was compensated to zero.

The plateau formation tendency observed in Fig. 6 (left), which is more evident in longer time period, is caused by the total DO concentration decrease due to the corrosion process. Lower the pH

value, shorter the linear part of the curve, because the *Acidithiobacillus ferrooxidans* metabolism is optimized for pH 1.4 and the bacteria catalyzed the iron oxidation more intensively at low pH values provoking thus more rapid DO concentration decrease. As a result the DO concentration gradient which is the moving force of the DO diffusion to the corroding specimen decreases and hence the DO consumption rate decrease as well, causing the plateau appearing tendency. The solution volume of 5 liters and the initial DO concentration excess of 11.8 mg $L^{-1}$ however is sufficient to ensure reliable results since the maximal DO consumption rate was determined to be only 4.372 mg $L^{-1}$ hour.

The MIC rate was evaluated by the slope of the DO concentration vs. time curve calculating the Fe oxidation rate corresponding to this DO consumption for every pH value. For pH 5 for example the oxygen consumption rate was found to be 0.033 mg $L^{-1}$ $h^{-1}$ determined by the slope $\mu_5$ of the DO consumption vs. time curve (Fig. 6, right), and the calibration curve presented in Fig. 2 right.

**Table 3**. Clark probe curves slopes and MIC rate of UNS G1020 in acid media with pH from 2 to 6 ($H_2SO_4$)

| pH | DO Consumption $mg_{O2}$ $L^{-1}$ $h^{-1}$ | MIC rate mm $y^{-1}$ | Corrosion Acceleration times |
|---|---|---|---|
| 2 | 4.372 | 8.68 | 4.91 |
| 3 | 1.028 | 1.99 | 3.47 |
| 4 | 0.097 | 0.19 | 2.71 |
| 5 | 0.033 | 0.067 | 1.80 |
| 6 | 0.008 | 0.017 | 1.16 |

Than taking into account that 1 mol of the DO oxidizes 4 moles of $Fe^{2+}$ (Eq. 9), one can obtain for the corrosion rate the value of 1.45 g $m^{-2}$ day, which applying the conversion coefficient of 0.0463 [51] yields 0.067 mm $year^{-1}$. Al the results obtained by this way at room temperature and optical density 0.15 (at 400 nm) of the bacterial culture of *Acidithiobacillus ferrooxidans* are presented in Table 3. Data displayed there showed that the MIC rate strongly depends on pH, since the bacteria metabolism strongly depend on pH.

The corrosion acceleration at pH 6 was found to be only 1.13 times while at pH 2 the corrosion acceleration was more than 4 times higher: 4.9 times. Since this study is related to MIC determination in non stirred aqueous media, it can serves as a reference for future study of the corrosion acceleration by MIC at stirred media at aerobic conditions.

## 4. CONCLUSIONS

The Clark amperometric oxygen sensor was applied for specific microbially induced corrosion (MIC) rate determination promoted by the bacterial strain *Acidithiobacillus ferrooxidans* accelerating the corrosion process. The corrosion acceleration of UNS G1020 carbon steel provoked by the bacteria in aqueous media with pH from 2 to 6 ($H_2SO_4$) was evaluated by the slope of the Clark sensor current

vs. time curves registered in the presence of bacteria after background subtraction. The Potentiodynamic Polarization was applied for general corrosion rate determination at abiotic conditions and the results were used as a reference for the determination of the corrosion acceleration provoked by the bacteria.

Values from 0.017 to 8.68 mm year$^{-1}$ were obtained for the bacterial corrosion rate provoked by the bacterial strain *Acidithiobacillus ferrooxidans* in the mentioned pH interval, while the general corrosion rates were in the range from 0.0147 to 1.766 mm year$^{-1}$ respectively, which represents corrosion acceleration between 1.16 and 4.91 times for the pH in the range from 6 to 2 respectively in unstirred aqueous media.

## References


1. M.J. Hernández Gayosso, G. Zavala Olivares, R. García Esquivel, J.L. Mora Mendoza and A.A. Padilla Viveros. *NACE Congress 2004*, paper 04589
2. F. Mansfeld and B. Little, *Corrosion Science*, 32 (1991) 247
3. S.C. Dexter, D.J. Duquette, O.W. Siebert and H.A. Videla, *Corrosion*, 47 (1991) 308
4. H.A. Videla, *Manual of Biocorrosion*, CRC Lewis Publishers, USA, (1996)
5. J.J. Santana1, F.J. Santana1, J.E. González1, R.M. Souto, S. González, J. Morales, *Int. J. Electrochem. Sci.*, 7 (2012) 711 - 724
6. *C. A. Loto, Int. J. Electrochem. Sci.*, 7 (2012) 9248 - 9270
7. S.C. Dexter, (Ed.), *Biologically Induced Corrosion*, NACE-8, Houston, TX: National Association of Corrosion Engineers, USA, (1986)
8. C.A.C. Sequeira and A.K. Tiller (Eds.), *Microbial Corrosion-1*, Elsevier Applied Science, New York, (1988)
9. C.A.C. Sequeira and A.K. Tiller (Eds.), Microbial Corrosion, *Proceedings of the 2$^{nd}$ EFC Workshop, European Federation of Corrosion Publications*, Number 8, The Institute of Materials, London, (1992)
10. C.A.C. Sequeira and A.K. Tiller (Eds.), Microbial Corrosion, *Proceedings of the 3$^{rd}$ EFC Workshop, European Federation of Corrosion Publications*, Number 15, The Institute of Materials, London, (1995)
11. H.A. Videla, *Manual of Biocorrosion*, Lewis Publishers, (1996)
12. G.G. Geesey, Z. Lewandowski and H.-C. Flemming (Eds.), *Biofouling and Biocorrosion in Industrial Water Systems*, Lewis Publishers, (1994)
13. J.R. Kearns and B.J. Little (Eds.), *Microbiologically Influenced Corrosion Testing*, American Society for Testing and Materials, Philadelphia, PA, USA, (1994)
14. B. Little, P. Wagner and F. Mansfeld, *International Materials Revie*, 36 (1991) 253
15. R. Zuo, E. Kus, F. Mansfeld and T. Wood, *Corrosion Science*, 47 (2005) 279
16. F.K. Sahrani, Z. Ibrahim, M. Aziz and A. Yahya, *Sains Malaysian*, 38 (2009) 359
17. C.A. Schnaitman, M.S. Korczynski, D.G. Lundgren, *Journal of Bacteriology*, 99 (1969) 552
18. O. Lowry, N. Resenbrough, A. Farr and R. Randall, *Journal of Biological Chemistry*, 193 (1951) 265
19. W.J. Ingledew, *Biotechnology and Bioengineering Symposium*,16 (1986) 23
20. D. Karamanev and L. Nikolov, *Bioprocess and Biosystems Engineering*, 6 (1991) 127
21. A. Avakyan and G. Karavaiko, *Microbiologia*, 39 (1970) 855 (in Russian).
22. W.J. Ingledew, *Biochimica et Biophysica Acta*, 683 (1982) 89
23. B. Vu, M. Chen, R.J. Crawford and E.P. Ivanova, *Molecules*,14 (2009) 2535
24. M. Schrenk, K. Edwards, R. Goodman, R. Hamers and J. Banfield, *Science*, 279 (1998) 1519

25. J. Duan, S. Wu, X. Zhang, G. Huang, M. Du and B. Hou, *Electrochimica Acta*, 54 (2008) 22
26. T. Brock and M. Madigan, *Microbiologia*, 6th Edition, Prentice Hall Hispanoamericana S.A., (1987)
27. S. Li, Y. Zhang, J. Liu and M.Yu, *Acta Physico-Chimica Sinica*, 24 (2008) 1553
28. H. Kanematsu, H. Ikigai, Y. Kikuchi and T. Oki, *Transactions of the Institute of Metal Finishing*, 83 (2005) 205
29. D.M. Drazic, *Modern Aspects of Electrochemistry*, No. 19, Plenum Press, New York, (1989), p. 69
30. I.-H. Plonski, *Modern Aspects of Electrochemistry*, No. 29, Plenum Press, New York, (1996), p. 203
31. J. O'M Bockris and D. Drazic, *Electrochim Acta*, 4 (1961) 325
32. J. O'M Bockris and H. Kita, *J. Electrochem Soc.*, 108 (1961) 676
33. J. O'M Bockris and D. Drazic, *Electrochim Acta*, 7 (1962) 293
34. B. Pesic and V.C. Storhok, CORROSION 2001, March 11-16, 2001, Houston, Tx, Conference Paper Document ID 01255, NACE International, (2001)
35. N. Lazaroff, *Journal of General Microbiology*, 101 (1977) 85-91.
36. M. Stoytcheva, B. Valdez, R. Zlatev, M. Schorr, M. Carrillo, Z. Velkova, *Advanced Materials Research*, 95 (2010) 73
37. http://www.globalmetals.com.au/_pdf/Black_Carbon_Steel/Black_Carbon_Steel_1020.pdf
38. J.-P. Magnin, F. Baillet, A. Boyer, R. Zlatev, M. Luca, A. Cheruy, and P. Ozil, *Canadian Journal of Chemical Engineering*, 76 (1998) 978
39. R. Zlatev , B. Valdez, M. Stoytcheva, R. Ramos and S. Kiyota, *Int. J. Electrochem. Sci*., 6 (2011) 2746
40. O.H. Tuovinen and D.P. Kelly, *Archives of Microbiology*, 98 (1974) 351
41. G. Charlot, *Les méthodes de la chimie analytique*, Masson, Paris (1961)
42. B. Pesic, D.J. Oliver and P. Wichlacz, *Biotechnology and Bioengineering*, 33 (1989) 428
43. Y. Tanji, A. Soejima, Y. Morono and H. Unno, *Kogaku Shinpojiumu Shirizu*, 70 (1999) 77
44. T. Bott, Biofilm and MIC monitoring, *Meeting of Task 5*, Venezia, Italy, April 13 (2000)
45. B. Tribollet, Biofilm and MIC monitoring, *Meeting of Task 5*, Venezia, Italy, April 13 (2000)
46. R. Zlatev, J.-P. Magnin, P. Ozil and M. Stoytcheva, *Biosensors and Bioelectronics*, 21 (2006) 1753
47. G. Sauerbrey, *Zeitschrift für Physik*, 155 (1959) 206
48. Trevor M. Letcher (2007). *Developments and applications in solubility* (1st ed.). Royal Society of Chemistry. p. 71.
49. M. Stoytcheva, R. Zlatev, J-P Magnin, M. Ovalle, B. Valdez, *Biosensors and Bioelectronics* 25 (2009) 482
50. A. Kopliku and D.L. Condanni, European Petroleum Computer Conference, Aberdeen, United Kingdom, 15-17 March (1994)
51. http://www.corrosion-doctors.org/Principles/Conversion.htm